

Land use/land Cover Change Detection in Tehran City Using Landsat Satellite Images

Mohammad Hamed Saeifar^{1*}, Mousa Mohammadnia²

¹Ph.D. Student in Remote Sensing, Afagh Research Institute, Iran University of Science and Technology, Tehran, Iran

²Researcher in Computer Science, Iran University of Science and Technology, Tehran, Iran

Received: May 6, 2015

Accepted: October 18, 2015

ABSTRACT

Land cover is changing rapidly over time. Detection of changes in ground surface would be of utmost importance in monitoring of land use/land cover (LULC) and in analyzing the spatiotemporal pattern of the changes. The overall objective of this study is to map the spatiotemporal changes of LULC using Landsat5 TM and Landsat8 (Operational Land Imager (OLI) sensor) in Tehran City. For this, supervised classification and Maximum Likelihood Method were used to map the LULC in the study area. According to which, the city was classified into six major classes. SPOT satellite images dating back to 2010 were used to check the accuracy of classification using Kappa Coefficient. As the results show, the overall accuracy and kappa coefficient values were 93.4103% and 0.9166 in 2010 and 98.8604% and 0.9858 in 2014. The results of post-classification techniques revealed that, from 2010 to 2014, the water bodies increased by 0.85 Km². This is mainly due to construction of an artificial lake in western Tehran converting bare lands to water bodies. The results also indicate that from 2010 to 2014, green spaces reduced by 62.80 km² and built-up areas increased by 12.86 km². It was obviously remarkable that built-up areas and manmade features have been expanded within the period of 2010-2014. In overall, increased population growth and rapid immigration rate to the city would be two main reasons for expansion of built-up areas and decreased area of green spaces and vegetation cover.

KEYWORDS: Land use/land cover, Change detection, Landsat, Post-Classification, Accuracy Assessment

1. INTRODUCTION

Tehran has faced significant structural changes in urban fabric so that regular seasonal and annual monitoring is required to detect the changes occurred over time. Urbanization and urban expansion can cause considerable changes in land use/land cover (LULC) patterns, which can impose negative impacts on urban areas, especially on green spaces, farmlands, vegetation cover, and natural environment [1].

Monitoring and detection of changes would be possible and facilitated by remote sensing technology. Generally speaking, remote sensing has found wide applications in a variety of research areas, such as LULC change detection [2,3], disaster management [4,5], vegetation cover change detection [6,7], urban expansion [8], and hydrology [9].

Change detection techniques based on multi temporal satellite images could track any kind of LULC changes occurred by natural and/or anthropogenic activities [10].

Change detection, as defined by Singh [11], is a process of recognizing changes in the state of an object or phenomenon by observing images at different times. Currently LULC mapping is considered a standard way to monitor spatiotemporal changes. In a research by Forkuo et al. (2012) changes in forest cover was detected to find the extent of LULC changes over time and space. Their findings quantified the LULC changing patterns around the catchments of the Owabi Dam. They emphasized on the potential of multi-temporal satellite data in mapping LULC spatiotemporal changes [12].

Remote sensing techniques are widely applicable in LULC mapping and change analysis. The remotely sensed data has become a major data source for change detection studies because of their high temporal frequency and repetitive coverage, their digital format which is suitable for computation and selective and wide spatial and spectral resolutions [13, 14, 15].

According to the latest consensus on 2012, Tehran has a population of over around 8.4 million inhabitants and is considered as the most densely populated city of Iran. Rapid rural-urban migration and population growth in the city have significantly influenced urban fabric so that in recent years the area of green space is increasingly being

*Corresponding Author: Mohammad Hamed Saeifar, Ph.D. Student in Remote Sensing, Afagh Research Institute, Iran University of Science and Technology, Tehran, Iran. Email: mh.saeifar@gmail.com;

less and land use change is happening on a large scale in the city. Rapid and excessive expansion of Tehran in recent decades lacks a firm sustainable basis. This would be the root-cause for many socio-economic problems among citizens as well as lots of environmental adverse consequences. Reducing the size of natural and herbal coatings has led to changes in regional climatic conditions. As the most basic fundamental step in this regard, it is essential to identify and quantify the land use changes over time and in different locations in order to clarify the direction of urban expansion. Further, it can also be determined that which land uses have had more changes than others. According to which, extend of land use changes over time would be quantified and managed. Given the importance of the issue, given the importance of the issue, the present study was carried out to detect spatiotemporal changes in LULC of Tehran City over a period of 2010-2014. The primary objective of this study was to identify the percentage of changes in different land uses in Tehran within the recent 4-year period based on remotely-sensed data. The findings of this research will clarify which land uses has undergone the greatest changes.

2. MATERIALS AND METHODS

The present study was performed in 6 steps, including identification of the study area, data collection, image pre-processing, supervised classification, data accuracy analysis, and change detection. Figure 2 shows the overall procedure of the methodology for detection of LULC changes in Tehran City over 2010 to 2014.

2.1. Study area

Tehran, as the capital city of Iran, is geographically situated between the latitudes of $35^{\circ}33'10''$ - $35^{\circ}33'10''$ N and the longitudes of $51^{\circ}05'17''$ - $51^{\circ}37'36''$ E. Including nearly 7 million inhabitants over an area of 730km^2 , it is among the most populous and the largest cities in Iran. The city has an average elevation of about 1600 m above the sea level.

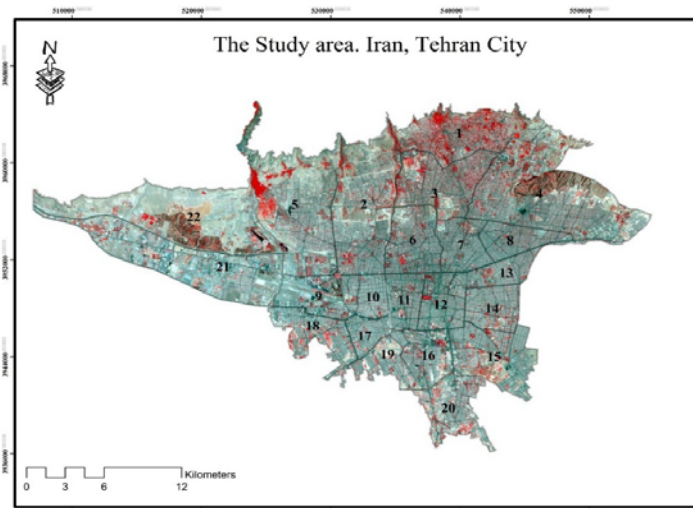


Figure1. Administrative division of Tehran City including 22 districts

2.2. Data Set

A 30 m spatial resolution Landsat-5 TM image acquired on 07 August 2010 and a Landsat-8 OLI image acquired on 18 August 2014 were used to map LULC changes in the study area (Figure 1). TM images are acquired in six spectral bands with a spatial resolution of 30 m. It is worth mentioning that the thermal band has a spatial resolution of 120 m did not used in this study [16, 17]. Landsat-images 8 (OLI sensor) have 8 spectral bands with a spatial resolution of 30 m, one panchromatic band with a spatial resolution of 15 m, and two thermal bands with a spatial resolution of 100 m which did not used in this study.

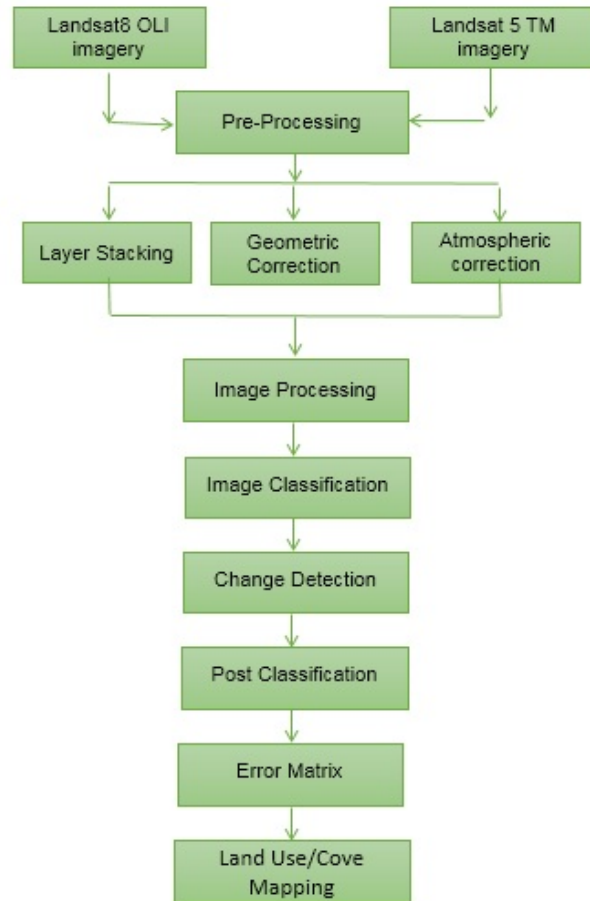


Figure 2. Flowchart of research procedure

Table 1. Specifications of Landsat TM, ETM+, and OLI data

Satellite	Sensor	Path/Row	Year	Resolution (m)
Landsat-5	TM	164/35	2010	30
Landsat-8	OLI	164/35	2014	30

2.3. Preprocessing of images

After atmospheric correction of satellite data, in order to prepare them for accurate and meaningful change detection, it was necessary to rectify the images geometrically [18].

The accuracy of image registration is usually explained in terms of Root-Mean-Square (RMS) error. The reasonable RMS error for Landsat TM imagery is about 0.5 pixels.

Landsat 5 TM and Landsat 8 OLI images downloaded from the U.S. Geological Survey (USGS) were geometrically registered to a 1:25000 digital topographic map. The projection system of the images was set to UTM WGS1984 Zone 39 N projection to ensure all data are geometrically co-locatable. The analysis results revealed that Landsat TM image, dating back to 2010, had a RMSE of 0.02 pixels and the Landsat OLI image had a RMSE of 0.03 pixels. The study area was masked from the full scene.

Among a variety of change detection methods developed so far [19], the post-classification comparison was used in this study to clarify and detect LULC changes.

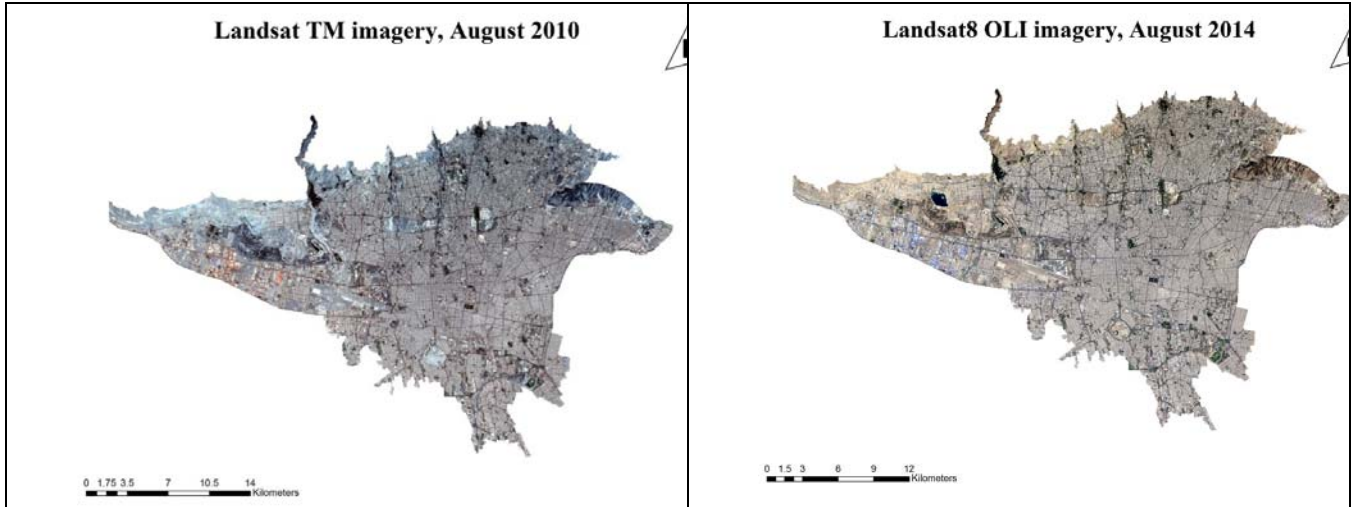


Figure 3. Satellite images of Tehran in 2010 and 2014

2.4. Classification of images

Generally, there are two procedures for image classification, namely unsupervised and supervised classification methods, which are used by image analysts. In unsupervised classification methods, some clusters are separated on the images by software based upon their reflectance values. In contrast, in supervised image classification methods, some areas of image are defined as training samples, each of which represents a particular feature on the earth. After defining a signature for each land cover types, the entire image will be classified based on the pre-defined signatures [20]. In this research, supervised classification was done by maximum likelihood decision rule.

Maximum likelihood method assumes that the statistics for each class in each band follow a normal distribution and a given pixel belongs to a specific class. Once specifying probability thresholds, all pixels will be classified. Each pixel is assigned to a class with the highest probability (maximum likelihood). If the highest probability of a pixel falls smaller than the predefined threshold; then that pixel will remain unclassified [21].

Maximum likelihood classification is implemented by calculating the following discriminant functions for each pixel in the image:

$$g_i(x) = \ln p(\omega_i) - \frac{1}{2} \ln |\Sigma_i| - \frac{1}{2} (x - m_i)^T \Sigma_i^{-1} (x - m_i) \quad \text{Eq. 1}$$

Where:

I = class

x = n-dimensional data (where n is the number of bands)

p(ω_i) = probability that the class ω_i occurs in the image and the same is assumed for all other classes

|\Sigma_i| = determinant of the covariance matrix of the data in the class ω_i

\Sigma_i⁻¹ = the inverse matrix

m_i = mean vector

In this research, the study area was classified into 6 land cover types based on the ground truth samples. The LULC classes include bareland, forest park, green spaces, built-up areas (cities, towns, and infrastructure), water bodies, and asphalt roads. The results of image classification by maximum likelihood method are shown in Figures 4 and 5.

2.5. Accuracy assessment of classification

Error matrix was used to evaluate the classification accuracy of the satellite images used in this study as a data set. Tables 2 and 3 show the number of points selected for each class and the classification accuracy. Producer accuracy indicates classification precision of pixels related to a particular class on the ground control map. In other word, it remarkably addresses the probability of miss-assigning of a pixel to a class.

User accuracy also indicates the probability of classification of a LULC class with the same class on the ground truth map.

The supervised classification in this study was done using training samples. Further, SPOT satellite images dating back to 2010 were used to check the accuracy of classification. The obtained results revealed an overall accuracy of 1375/1472 (93.4103%) and Kappa Coefficient of 0.9166 for the images taken in 2010. As for the images

taken in 2014, the overall accuracy and Kappa Coefficient were estimated to be 1735/1755 (98.8604%) and 0.9858, respectively (Tables 2 and 3).

Kappa coefficient is an accuracy indicator derived from error matrix. It calculates the classification accuracy compared to a random assortment. In better words, Kappa values reflect classification accuracy compared to the case when an image is totally classified randomly (eg. unsupervised classification) [22].

Kappa is widely used in accuracy analysis because it not only involves the items on the main diagonal but also engages all items in the error matrix. Accordingly, all of the items in the error matrix, not only those on the main diagonal, could contribute in accuracy analysis [23].

Kappa values are categorized into 3 groups: a value greater than 0.80 (80%) represents strong agreement, a value between 0.40 and 0.80 (40 to 80%) represents moderate agreement, and a value below 0.40 (40%) represents poor agreement [24]. According to Jensen and Cowen [25], Kappa is computed using Equation (2).

$$K = \frac{N \sum_{i=1}^R X_{ii} - \sum_{i=1}^R (X_{i+} X_{+i})}{N^2 - \sum_{i=1}^R (X_{i+} X_{+i})} \quad \text{Eq.2}$$

Where:

N= total number of sites in the matrix,

R= number of rows in the matrix,

X_{ii}= value in the ith row and ith column,

X_{+i} = total value for the ith row, and

X_{i+} = total value for the ith column

The accuracy level and kappa vlaues are summarized in Table 2 and 3.

Table 2. Error Matrix of TM images, 2010

Classes	Forest park	Bare land	Green space	Water bodies	Built-up area	Asphalt surface	Total	User Accuracy
Forest Park	72	1	2	0	0	1	76	94.74
Bare Land	0	351	0	0	6	3	360	97.50
Green Space	52	0	346	0	0	0	398	86.93
Water bodies	0	0	0	104	0	0	104	100
Built-up area	0	5	0	0	361	0	366	98.63
Asphalt surface	2	19	0	2	4	141	168	83.93
Total	126	376	348	106	371	145	1472	-
Producer Accuracy	57.14	93.35	99.43	98.11	97.30	97.24	-	-

Overall Accuracy = (1375/1472) 93.4103% Kappa Coefficient = 0.9166

Table 3. Error Matrix of OLI 2014

Class	Forest park	Bare land	Green space	Water bodies	Built-up areas	Asphalt surface	Total	User Accuracy
Forest park	370	0	0	0	0	0	370	100.00
Bare land	1	377	0	0	5	1	384	98.18
Green space	9	0	374	0	0	0	383	97.65
Water bodies	0	0	0	94	0	0	94	100.00
Built-up areas	1	0	0	0	379	1	381	99.48
Asphalt surface	0	0	0	1	1	141	143	98.60
Total	381	377	374	95	385	143	1755	-
Producer Accuracy	97.11	100.00	100.00	98.95	98.44	98.60	-	-

Overall Accuracy = (1735/1755) 98.8604% Kappa Coefficient = 0.9858

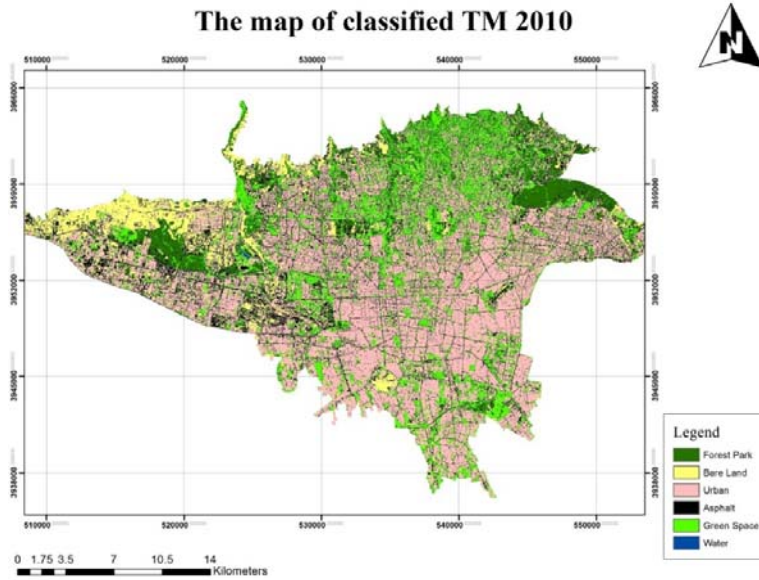


Figure 4. LULC classifications on TM images, 2010

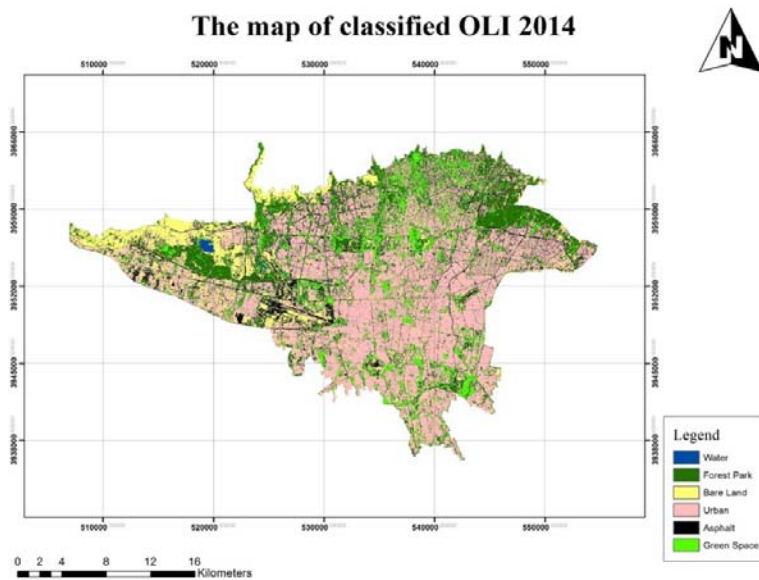


Figure 5. ULC classification on OLI images, 2014

3. RESULTS AND DISCUSSIONS

The satellite images were classified using Maximum Likelihood method into 6 classes, including bare land, forest park, green space, built-up areas (cities, towns, and infrastructure), water bodies, and asphalt surface. Afterwards, the accuracy of classification was checked using error matrix and Kappa coefficient for both Landsat TM 2010 and Landsat OLI 2014 images, which the obtained results are presented in Tables 2 and 3. Accordingly, LULC changes in the study area were detected using post-classification comparison method as a commonly used change detection technique. According to which, the LULC maps were compared pairwise to track the area of land use changes (Table 4). The final results revealed that how the different land use classes have been changed within the study period [26].

As Table 4 suggests, the values in the total column indicate the total number of pixels in the base LULC map (initial state class) while the values in the total row represent the total number of Pixels in the final LULC map (final

state class). The total column is simply a class-by-class summation of all final state pixels that fell into the selected Initial State classes.

The changing area row indicates the total number of initial state pixels changed over time. The difference row quantifies the difference in total number of each land use class in two LULC images, computed by subtracting the sum of initial state class from that of the final state class. The positive value in the difference row indicates increased area of a given land use. According to the research objective, medium resolution data was required to track land use changes. Therefore, Landsat images were used in this study. There was no need to use higher resolution data to show further details. As another main objective in this research, capability of the remote sensing technique in preparation of LULC maps and classification of different land uses was investigated. In this research, a total number of 6 land use classes were identified. Further, the accuracy of LULC maps was checked using SPOT images dating back to 2010. Error matrix for each land use class is given in Tables 2 and 3. The LULC changes could be detected using two LULC maps as well as the initial-final state matrix (Figs. 4, and 5 and Table 4).

According to Figure 6 and Table 4, the area of built-up regions was 256.73 km² in 2010 and 269.59 km² in 2014 which constitute 43% and 45% of the entire study area, respectively. In other words, the area of built-up regions has expanded for 128.6 ha over the study period. The expansion of the built-up area mainly occurred in the central, western, southern, and eastern parts as the most populous areas in the city. The area of green spaces has decreased by 62.8 km² as a result of expansion of built-up areas and bare lands within the study period. An increase of 0.85 km² in the area of water bodies was due to construction of an artificial lake in western part of the study area which could easily be detected in the LULC map of the year 2014. Forest parks as a part of the LULC map have increased by 2% in these years in the study area.

Table 4. Post-classification of different land use classes in Tehran City

Land use classes	Forest park Km ²	Bare land Km ²	Built-up area Km ²	Asphalt surface Km ²	Water bodies Km ²	Green spaces Km ²	Total (base map) Km ²	Total Km ²
Forest park	34.88	2.35	3.06	8.38	0.00	25.83	74.51	74.51
Bare land	7.54	46.20	33.79	30.65	0.04	6.78	125.00	125.00
Built-up area	5.32	6.63	199.41	36.03	0.00	22.19	269.59	269.59
Asphalt surface	2.71	1.80	19.23	23.83	0.00	24.82	72.49	72.49
Water bodies	0.37	0.59	0.00	0.02	0.14	0.03	1.13	1.13
Green space	12.76	1.47	1.22	1.38	0.02	33.49	50.35	50.35
Total (final map)	63.59	59.04	256.73	100.29	0.28	113.15	0.00	0.00
Changing area	28.71	12.84	57.31	76.45	0.14	79.65	0.00	0.00
Difference	10.92	65.92	12.86	-27.80	0.85	-62.80	0.00	0.00

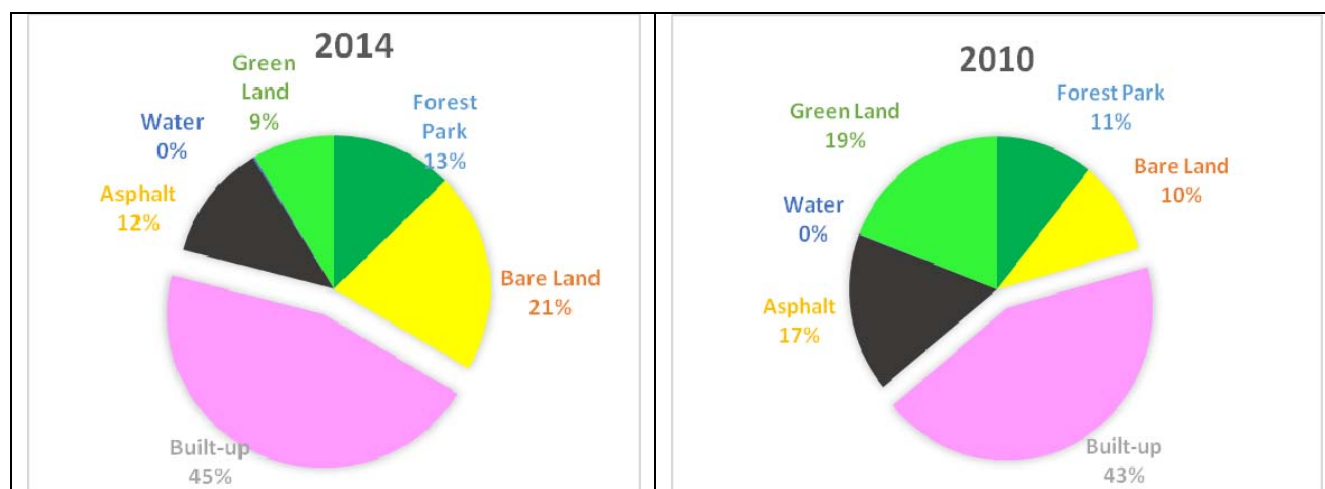


Figure 6. Area of different land use classes in 2010 and 2014

In a research by Yaghoubkhani in 2012 on land use changes of Tehran City, residential land, urban built up areas, and industrial lands were introduced as land uses with the greatest increase over a 20-year period (1986–2006). This is in line with the results of this study. According to the results, built-up areas have been expanded for 128.6 ha over the study period [27]. Golmehri in 2008 reported similar results [28]. Arsanjani et al. (2013) stimulated spatiotemporal development of Tehran City by the year 2026. They confirmed the expansion of built-up areas in the city and predicted that this expansion will be in future in the northwestern part of Tehran, continuing toward the south along the interchange networks [29]. Talebi in 2011 studied the changing area of green space in Tehran over the years 1988-2009. He reported loss of per capita green area from 22 m in 1988 to 18 m in 2009 [30]. The declined area of green spaces in Tehran was also confirmed by the present study. According to which, the area of green spaces was decreased by 62.8 km² within the study period.

4. CONCLUSION

The use of satellite images is one the most useful approaches for monitoring spatiotemporal changes particularly environmental and LULC changes. Landsat images can be used to map perfectly land cover changes and to analyze changing trends. This study was carried out to track spatiotemporal LULC changes in Tehran over a period of 2010 to 2014.

Post-classification, as one of the change detection techniques was used to detect LULC changes in Tehran, particularly those changes in some of the LULC classes such as water bodies and bare lands, using by Landsat TM and Landsat8 (OLI sensor) from 2010 to 2014.

For this, LULC changes in the study area were detected by supervised classification of satellite images using maximum likelihood method. The accuracy of classification was checked by SPOT images dating back to 2010.

Accordingly, major identified LULC classes include a total number of 6 classes of bare soil, built-up areas, green spaces, water bodies, forest parks, and asphalt roads. It was obviously remarkable that built-up areas and manmade features have been expanded within the period of 2010-2014.

Such an increase in the mentioned classes was mainly due to physical expansion of Tehran in these years caused many problems such as decreased area of green spaces and vegetation cover in the city.

As the obtained results show, the use of Landsat data and maximum likelihood algorithm in supervised classification can lead to a detailed mapping of changes with a suitable accuracy.

In overall, increased population growth and rapid immigration rate to the city would be two main reasons for expansion of built-up areas and decreased area of green spaces and vegetation cover.

REFERENCES

1. Long, H., X. Wu, W. Wang and G. Dong, 2008. Analysis of urban-rural land-use change during 1995-2006 and its policy dimensional driving forces in Chongqing, China. *Sensor.*, 8(2): 681-699.
2. Salmon, B. P., W. Kleynhans, F. van den Bergh, J. C. Olivier, T. L. Grobler and K. J. Wessels, 2013. Land covers change detection using the internal covariance matrix of the extended Kalman filter over multiple spectral bands. *IEEE J. Sel. Top. Appl.*, 6(3): 1079-1085.
3. Demir, B., F. Bovolo and L. Bruzzone, 2013. Updating land-cover maps by classification of image time series: A novel change-detection-driven transfer learning approach. *Geosci. Remote Sens. IEEE Trans.*, 51(1): 300-312.
4. Volpi, M., G. P. Petropoulos and M. Kanevski, 2013. Flooding extent cartography with Landsat TM imagery and regularized kernel Fisher's discriminant analysis. *Comput. Geosci.*, 57: 24-31.
5. Brisco, B., A. Schmitt, K. Murnaghan, S. Kaya, and A. Roth, 2013. SAR polarimetric change detection for flooded vegetation. *Int. J. Digital Earth*, 6(2): 103-114.
6. Kaliraj, S., S. M. Meenakshi and V. K. Malar, 2012. Application of Remote Sensing in Detection of Forest Cover Changes Using Geo-Statistical Change Detection Matrices- A Case Study of Devanampatti Reserve Forest, Tamilnadu, India. *Nat. Environ. Pollut. Technol.*, 11(2): 261-269.
7. Markogianni, V., E. Dimitriou and D. P. Kalivas, 2013. Land-use and vegetation change detection in Plastira artificial lake catchment (Greece) by using remote-sensing and GIS techniques. *Int. J. Remote Sens.*, 34(4): 1265-1281.
8. Bagan, H. and Y. Yamagata, 2012. Landsat analysis of urban growth: How Tokyo became the world's largest megacity during the last 40 years. *Remote Sens. Environ.*, 127: 210-222.

9. Raja, R. A., V. Anand, A. S. Kumar, S. Maithani and V. A. Kumar, 2013. Wavelet based post classification change detection technique for urban growth monitoring. *J. Indian Soc. Remote.*, 41(1): 35-43.
10. Rokni, K., A. Ahmad, A. Selamat and S. Hazini, 2014. Water feature extraction and change detection using multitemporal Landsat imagery. *Remote Sens.*, 6(5): 4173-4189.
11. Fuller, R. M., G. M. Smith and B. J. Devereux, 2003. The characterisation and measurement of land cover change through remote sensing: problems in operational applications. *Int. J. Appl. Earth Obs.*, 4(3): 243-253.
12. Singh, A. 1989. Review article digital change detection techniques using remotely-sensed data. *Int. J. remote sens.*, 10(6): 989-1003.
13. Forkuo, E. K. and A. Frimpong, 2012. Analysis of forest cover change detection. *Int. J. Remote Sens. Application*, 2(4): 82-92.
14. Chen, G., G. J. Hay, L. M. Carvalho and M. A. Wulder, 2012. Object-based change detection. *Int. J. Remote Sens.*, 33(14): 4434-4457.
15. Wulder, M. A. and S. E. Franklin, 2006. *Understanding Forest Disturbance and Spatial Pattern: Remote Sensing and GIS Approaches*. CRC Press, pp: 31.
16. Lunetta, R. S., D. M. Johnson, J. G. Lyon and J. Crotwell, 2004. Impacts of imagery temporal frequency on land-cover change detection monitoring. *Remote Sens. Environ.*, 89(4): 444-454.
17. Chander, G., B. L. Markham and D. L. Helder, 2009. Summary of current radiometric calibration coefficients for Landsat MSS, TM, ETM+, and EO-1 ALI sensors. *Remote sens. Environ.*, 113(5): 893-903.
18. Helder, D. L., S. Karki, R. Bhatt, E. Micijevic, D. Aaron, and B. Jasinski, 2012. Radiometric calibration of the Landsat MSS sensor series. *Geosci. Remote Sens., IEEE Trans.*, 50(6): 2380-2399.
19. H. Mahmoodzadeh, 2006. Digital Change Detection Using Remotely Sensed Data for Monitoring Green Space Destruction in Tabriz. *Int. J. Environ. Res.* 1 (1): 35-41
20. Wickware, G. M. and P. J. Howarth, 1981. Change detection in the Peace—Athabasca delta using digital Landsat data. *Remote Sens. Environ.*, 11: 9-25.
21. Coskun, H. G., U. Alganci, and G. Usta, 2008. Analysis of land use change and urbanization in the Kucukcekmece water basin (Istanbul, Turkey) with temporal satellite data using remote sensing and GIS. *Sensors*, 8(11): 7213-7223.
22. Richards, J. A. 1999. *Remote sensing digital image analysis*. Springer Berlin Heidelberg.
23. G. Foody, 1992. On the Compensation for Chance Agreement in Image Classification Accuracy Assessment. *Photogrammetric Engineering and Remote Sensing*, 58(10), 1459-1460 .
24. Rosenfield, G. & Fitzpatrick-Lins, K. (1986). A Coefficient of Agreement as a Measure of Thematic Classification Accuracy. *Photogrammetric Engineering and Remote Sensing*, 52(2), 223-227
25. Congalton, R. G. (1991). A review of assessing the accuracy of classifications of remotely sensed data. *Remote sensing of environment*, 37(1), 35-46.
26. Jensen, J. R., & Cowen, D. C. (1999). Remote sensing of urban/suburban infrastructure and socio-economic attributes. *Photogramm. Eng. Rem. S.*, 65: 611-622.
27. M. Yaghoubkhani, 2012. The Study of Land Use Changes in the Tehran Metropolitan Area by Using MOLAND Model. 48th ISOCARP Congress, Fast Forward – Planning in a (hyper) dynamic urban context, Perm, Russia.
28. E. Golmehr, 2008. A remote sensing evaluation for agronomic land use mapping in Tehran Province, Iran. *J. Appl. Sci. Environ. Manage.*, 12(2): 43–46.
29. Arsanjani J. J., M. Helbich, E. de Noronha Vaz, 2013. Spatiotemporal simulation of urban growth patterns using agent-based modeling: The case of Tehran. *Cities*, 32: 33–42.
30. Talebi M. R. 2011. Investigation of Tehran green Space changes and its role in air pollution Using LANDSAT images from 1980-2010. 5th SASTech 2011, Khavaran Higher Education Institute, Mashhad, Iran. May 12-14.